JEDI: A versatile code for strain analysis of molecular and periodic systems under deformation

Henry Wang,[1] Sanna Benter,[1] Wilke Dononelli,[2,3,4*] Tim Neudecker[1,3,4,*]

[1]University of Bremen, Institute for Physical and Theoretical Chemistry, Leobener Straße 6, D-28359 Bremen, Germany

[2]Hybrid Materials Interfaces Group, Am Fallturm 1, D-28359 Bremen, Germany

[3]Bremen Center for Computational Materials Science, Am Fallturm 1, D-28359 Bremen, Germany

[4]MAPEX Center for Materials and Processes, Bibliothekstraße 1, D-28359 Bremen, Germany

*Authors contributed equally. Corresponding authors. Email: wido@uni-bremen.de; neudecker@uni-bremen.de

Abstract: Stretching or compression can induce significant energetic, geometric and spectroscopic changes in materials. To fully exploit these effects in the design of mechano- or piezochromic materials, self-healing polymers, and other mechanoresponsive devices, a detailed knowledge about the distribution of mechanical strain in the material is essential. Within the past decade, the Judgement of Energy DIstribution (JEDI) analysis has emerged as a useful tool for this purpose. Based on the harmonic approximation, the strain energy in each bond length, bond angle and dihedral angle of a deformed system is calculated using quantum chemical methods. This allows the identification of the force-bearing scaffold of the system, leading to an understanding of mechanochemical processes at the most fundamental level. Here we present a publicly available code that generalizes the JEDI analysis, which has previously only been available for isolated molecules. Now the code has been extended to two- and three-dimensional periodic systems, supramolecular clusters, and substructures of chemical systems under various types of deformation. Due to the implementation of JEDI into the Atomic Simulation Environment (ASE), the JEDI analysis can be interfaced with a plethora of program packages that allow the calculation of electronic energies for molecular systems and systems with periodic boundary conditions. The automated generation of a color-coded three-dimensional structure *via* the Visual Molecular Dynamics (VMD) program allows insightful visual analyses of the force-bearing scaffold of the strained system.

1 Introduction

The mechanical deformation of a molecular material leads to structural changes at the atomic level in the form of modifications in the geometries of its constituent molecules or, in case a crystal is considered, its crystal lattice parameters. These mechanically induced geometric changes at the atomic level can give rise to spectroscopic signals, which can be exploited in the design of mechano-[1,2] and piezochromic[3–5] materials. Of particular interest in this regard are mechanophores, i.e., small molecular units that respond to mechanical deformation by profound structural changes such as bond rupture.[6–8] Embedded in a polymer, mechanical force that is transmitted from the strained macroscopic material to the mechanophore can give rise to a plethora of effects, such as molecular cargo release, self-healing or force-induced color changes.[9–13] Moreover, compression is known to lead to spin crossover in some transition metal complexes,[14–16] highlighting the influence of deformation on electronic properties. Practical applications of mechanochemistry in the manufacturing of tamper-proof packaging, the indication of loads in the construction industry, and the design of novel storage materials can be envisioned.

Experimentally, a plethora of methods is available to induce geometric changes in materials. Simple stretching or compression of functional polymers allows the activation of mechanophores.[17,18] In single-molecule force spectroscopy (SMFS),[19–22] setups like the Atomic Force Microscope (AFM) or optical or magnetic tweezers are used to apply stretching forces to biological macromolecules. In sonochemical setups, ultrasound generates stretching forces, high pressures and extreme temperatures that can be used to achieve activation of force-responsive polymers.[23–27] In ball mills, the impact of the metal balls generates tremendous deformations within the crushed materials, which are not always destructive, but which can be used for the creation of new covalent bonds as well.[28,29] Furthermore, the Diamond Anvil Cell (DAC) allows the application of hydrostatic pressure to molecular systems up to several hundred GPa, which is within the range of pressure at the center of the Earth.[30,31]

Considering the wealth of experimental techniques available for the deformation of materials and the futuristic applications pointed out above, it is unfortunate that a complete understanding of the influence of mechanical stress on the structural, energetic and spectroscopic properties of materials is still missing. While great progress has been made in the development of descriptive models of mechanochemistry,[32–36] which are often based on electronic structure calculations, the complexity of the experimental mechanochemical techniques and the inherent multiscale nature of mechanochemical transformations hampers the development of a general theoretical framework of mechanochemistry.

Among the most successful methodologies for the rationalization of mechanochemical events are

strain analysis tools.[32] These approaches allow the quantification of the distribution of mechanical stress within the deformed system.[37–39] A quantification of bond strengths, e.g., can be achieved by the calculation of compliance constants.[40–44] The Force Distribution Analysis (FDA) allows the analysis of pairwise forces and the identification of stress networks in biological systems.[45–49] For the case of inherently strained molecules, established methods like isodesmic and homodesmotic reactions[50] and the recently introduced StrainViz approach[51] enable strain localization, assessments of the stability of the strained molecules as well as predictions about their reactivity.

An alternative to these methods is the Judgement of Energy DIstribution (JEDI) analysis, which was introduced in 2014.[52,53] Based on the harmonic approximation and electronic structure calculations, a strain energy is assigned to each internal coordinate of a mechanically deformed system, i.e., each of its bond lengths, bond angles and dihedral angles. In the past, the JEDI analysis has been used to understand the mechanochemical properties of knotted polymer strands,[54,55] to investigate the possibility of force-induced retro-click reactions of triazoles,[56] to quantify the strain in adsorbates on a metal oxide surface,[57] to study mechanobiological events,[58] to judge the stability of inherently strained molecules,[59,60] and to rationalize the activation efficiency of various mechanophores.[61–63]

While these investigations have yielded valuable insights into diverse mechanochemical processes, the JEDI analysis has hitherto been limited to isolated molecules under stretching deformation. In this paper, we present a generalization of the JEDI analysis in two respects. First, the scope of the JEDI analysis is extended to substructures of chemical systems as well as to two- and three-dimensional, periodic materials. Second, various types of deformation, e.g., stretching and uniaxial or hydrostatic compression, can be modeled. We have implemented the JEDI analysis in the Atomic Simulation Environment (`ASE`)[64] to ensure compatibility with a wide range of electronic structure codes that are used to carry out the underlying electronic structure calculations.

The rest of the paper is structured as follows. After recapitulating the theoretical background of the JEDI analysis (Section 2), details on the implementation are given in Section 3. Subsequently, several examples on the use of the new, generalized implementation of the JEDI analysis are presented in Section 4. The purpose of these examples is not the generation of new insights in the mechanochemistry of various materials, but rather a demonstration of the wide range of molecules, materials and deformation modes that can be simulated with JEDI and the computer codes that can be interfaced with it. Finally, the conclusions are summarized and an outlook is given in Section 5.

2 Theory

In JEDI, a strain energy value is assigned to each internal coordinate of a mechanically deformed system, i.e., its bond lengths, bond angles and dihedral angles. The inclusion of all internal coordinates of the system leads to a redundant coordinate system. As shown previously,[53,65] the use of such redundant internal coordinates (RICs) is required for an insightful strain analysis and for a unique representation of the force-bearing scaffold. Only a brief overview of the theoretical background of the JEDI analysis shall be given here. The interested reader is referred to ref. 53 for a more detailed derivation. Similarly, only the electronic ground state is considered here. Strain analysis in the electronically excited state, with applications in photomechanochemistry, has been described elsewhere.[66,67]

The strain energy ΔE_i in one of the M internal coordinates of a mechanically deformed system is calculated by JEDI in the harmonic approximation as

$$\Delta E_i = \frac{1}{2} \sum_{j}^{M} \left. \frac{\partial^2 V(\vec{q})}{\partial q_i \partial q_j} \right|_{\vec{q}=\vec{q_0}} \Delta q_i \Delta q_j \ . \tag{1}$$

Here, $\left. \frac{\partial^2 V(\vec{q})}{\partial q_i \partial q_j} \right|_{\vec{q}=\vec{q_0}}$ are the elements of the Hessian matrix $\mathbf{H_q}$ in RICs at the strain-free reference geometry $\vec{q_0}$, and Δq_i is the strain-induced difference in internal coordinate i w.r.t. the relaxed reference geometry. While previous studies have predominantly focused on stretching forces that induce deformation in chemical systems, it is important to note that other types of mechanical load, e.g., compressive forces, can be used to induce deformations, with resulting Δq values being calculated in an analogous way.

Since electronic structure codes typically calculate the Hessian matrix not in RICs ($\mathbf{H_q}$), but in Cartesian coordinates ($\mathbf{H_x}$), it is necessary to carry out a coordinate transformation of the Hessian. For this, Wilson's B-matrix is used.[68] The elements of $\mathbf{B}$ are defined as

$$\mathbf{B}_{ij} = \frac{\partial q_i}{\partial x_j} \ , \tag{2}$$

i.e., they quantify the change in internal coordinate q_i when the Cartesian coordinate x_j is changed. The elements $\mathbf{B}_{ij}$, which are different for bond lengths, bond angles and dihedral angles, are given in ref. 69. Based on this work, we have added the possibility to analyze the strain in hydrogen bonds, where the elements of $\mathbf{B}$ are identical to those of regular covalent bonds.

Helgaker and Bakken have introduced the matrix $\mathbf{P}$, which is a projection matrix onto the range of $\mathbf{B}$,[69]

$$\mathbf{P} = \mathbf{B}\mathbf{B}^{+} \, , \tag{3}$$

where $\mathbf{B}^{+}$ is the generalized inverse or pseudoinverse of the (non-square) matrix $\mathbf{B}$. In JEDI, $\mathbf{B}^{+}$ is calculated using the `numpy` package.

The definition of $\mathbf{B}$ and $\mathbf{P}$ allows the transformation of the Hessian matrix in Cartesian coordinates, $\mathbf{H_x}$, into RICs *via*

$$\mathbf{H_q} = \mathbf{P}(\mathbf{B^t})^{+}\mathbf{H_x}\mathbf{B}^{+}\mathbf{P} \tag{4}$$

The strain energy of the entire chemical system can be obtained by summing over the energy contributions by each individual internal coordinate,

$$\Delta E_{\text{harm}} = \sum_{i}^{M} \Delta E_i = \frac{1}{2} \sum_{i,j}^{M} \left. \frac{\partial^2 V(\vec{q})}{\partial q_i \partial q_j} \right|_{\vec{q}=\vec{q_0}} \Delta q_i \Delta q_j \, , \tag{5}$$

resulting in the so-called "harmonic strain energy", since JEDI is based on the harmonic approximation. It is insightful to compare ΔE_{harm} to $\Delta E_{\text{ab initio}}$, the latter of which is the energy difference between the relaxed and the strained geometries calculated by electronic structure methods. This comparison allows a quantification of the error that is introduced by the harmonic approximation. Severe errors are typically found in systems with highly stretched bonds (where a method to mitigate this problem has been suggested before[56]), and in cases where torsional angles flip from one minimum on the potential energy surface to another. In these cases, the Δq_i values are exceedingly large, leading to unphysically high strain energies predicted by JEDI. Hence, a quantification of the error of the harmonic approximation by comparing ΔE_{harm} to $\Delta E_{\text{ab initio}}$ is always recommended.

The JEDI analysis requires electronic structure calculations of 1) the relaxed geometry of a chemical system, which is typically obtained by a standard geometry optimization, 2) the Hessian matrix in Cartesian coordinates, $\mathbf{H_x}$, at the relaxed reference geometry, and 3) a strained geometry. The latter can be obtained by quantum chemical methods that yield stretched[32] or compressed[70,71] geometries. The underlying electronic structure calculations are typically carried out using Density Functional Theory (DFT)[72,73] or wavefunction-based methods like Møller-Plesset Perturbation Theory[74] or the Coupled-Cluster approach.[75] The JEDI analysis carries out the transformation of $\mathbf{H_x}$ into $\mathbf{H_q}$, the calculation of the RICs and their mechanically induced changes as well as the calculation of the individual energy contributions ΔE_i (eq. 1) and the total harmonic strain energy ΔE_{harm} (eq. 5).

It has been shown previously that the JEDI analysis can also be used to calculate the distribution of strain energy dynamically within *ab initio* Molecular Dynamics (AIMD) simulations.[54,56] In this scenario, the JEDI analysis is carried out for each time step individually, and the structure found at a given time step is considered as a deformed geometry. An example of such a dynamical JEDI analysis is given in Section 4.5.

3 Implementation

The JEDI analysis has been implemented with the goal of maximum versatility. Several modes of deformation can be applied to either isolated molecular, supramolecular or periodic systems. For this purpose, a range of electronic structure programs that carry out the calculations of the relaxed and deformed geometries and the Hessian matrix are supported. This task is complicated by the diversity of input and output of the applied electronic structure codes, which would need to be read and processed by a standalone JEDI script. To solve these problems, the JEDI analysis was implemented in the Atomic Simulation Environment (`ASE`),[64] which is a `python` suite that interacts with a wealth of electronic structure codes, generates the required input and handles the output. The implementation of JEDI into `ASE` eliminates the problem of adapting the code to each individual system, deformation mode and code environment, allowing straightforward strain analyses based on a few lines of `python3.8` code. The JEDI code can be downloaded freely from `github` under the MIT license and extensive online tutorial material is available.[†]

The workflow of a typical JEDI analysis is shown in Scheme 1. Initially, electronic structure calculations with a user-defined program package and a computational method for the deformation of the system are carried out, which yield the geometries of the relaxed and strained systems and the Hessian matrix at the relaxed geometry. The relaxation and calculation of the Hessian can either be performed directly in the underlying electronic structure code or externally by `ASE`. Note, however, that `ASE` always calculates a numerical Hessian based on finite displacements, whereas most electronic structure codes have the possibility to calculate analytical Hessians for many electronic structure methods. While computationally more expensive than analytical calculations, a numerical calculation of the Hessian by `ASE` enables JEDI analyses with methods for which an analytical Hessian is not available.

An example for a JEDI script for a strain analysis of ethane, in which the carbon-carbon bond is

[†] https://github.com/neudecker-group/jedi

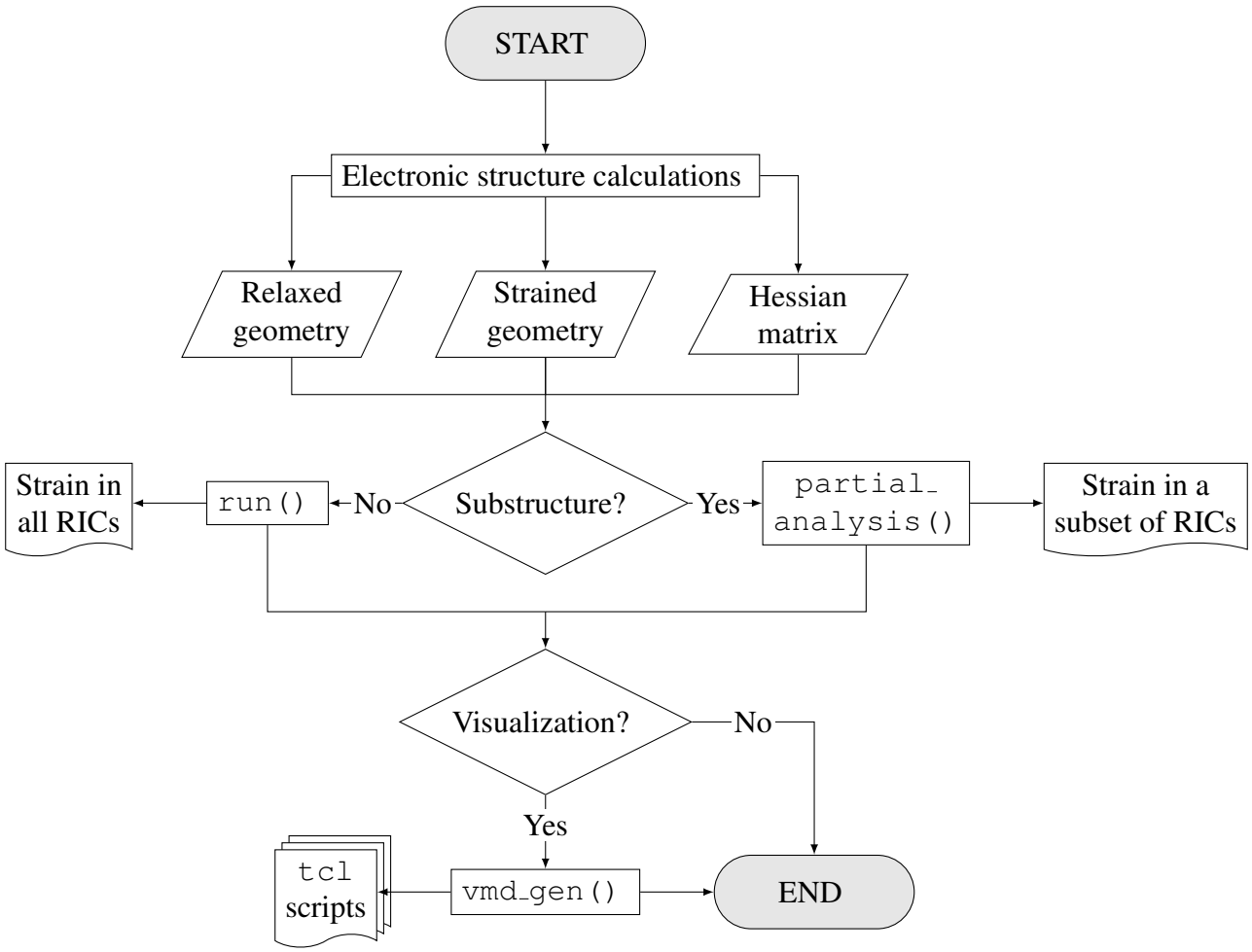

Scheme 1: Program workflow of the JEDI analysis. RICs: Redundant internal coordinates.

pulled apart, is shown here (cf. Section 4.1 for a discussion of the results):

```
from ase.build import molecule
from ase.visualize import view
from ase.calculators.orca import  ORCA
from jedi.io.orca import OrcaOptimizer, get_vibrations
from jedi.jedi import Jedi
mol=molecule('C2H6')



calc = ORCA(label='opt',
            orcasimpleinput='DLPNO-CCSD(T) cc-pVTZ cc-pVTZ/C TIGHTSCF
             ↪  OPT NumGrad'
```

```
            ,task='opt')
opt=OrcaOptimizer(mol,calc)
opt.run()


mol.calc=ORCA(label='orcafreq',
              orcasimpleinput='DLPNO-CCSD(T) cc-pVTZ cc-pVTZ/C TIGHTSCF
               ↪ FREQ',
              task='sp')
mol.get_potential_energy()
modes=get_vibrations('orcafreq',mol)

mol2=mol.copy()
calc = ORCA(label='stretch',
            orcasimpleinput='DLPNO-CCSD(T) cc-pVTZ cc-pVTZ/C TIGHTSCF
             ↪ OPT NumGrad',
            orcablocks='''%geom
    POTENTIALS
        { C 0 1 4.0 }
    end
end ''',task='opt')
opt=OrcaOptimizer(mol2,calc)
opt.run()

j=Jedi(mol,mol2,modes)
j.run()
j.vmd_gen()
```

If a strain analysis of the entire system is desired, the JEDI analysis is run normally. In this case, the RICs of the system are calculated by JEDI based on interatomic distances. If the distance between two atoms is smaller than 1.3 times the sum of covalent radii, a bond is defined between the two atoms. This default parameter can be changed by the user, however, in our tests it was never necessary to change the default to generate a chemically meaningful set of RICs. Any two adjacent bonds form a bond angle

	Strain energy (kcal/mol)	Deviation (%)			
Ab initio	3.17	-			
JEDI	3.86	21.73			
RIC No.	**RIC type**	**Indices**	**delta_q (a.u.)**	**Percentage**	**Energy (kcal/mol)**
1	Bond	C0 C1	0.000	0.0	0.00
...	...	...	...	...	...
9	Bond	C3 H14	0.189	100.0	3.86
...	...	...	...	...	...
24	Bond angle	C0 C1 C2	0.000	0.0	0.00
...	...	...	...	...	...
60	Dihedral angle	C5 C0 C1 C2	0.00	0.0	0.00
...	...	...	...	...	...

Table 1: Excerpt from an example JEDI analysis of biphenyl, in which one of the carbon-hydrogen bonds (internal indices: C3 and H14) is elongated. In the upper part of the table, the total strain energy of the system calculated by the electronic structure code ($\Delta E_{\text{ab initio}}$, "Ab initio") and by JEDI (ΔE_{harm}, "JEDI") as well as the deviation between $\Delta E_{\text{ab initio}}$ and ΔE_{harm} are listed. The columns below list (from left to right) the index of the RIC, the type of the RIC, the indices of the atoms involved in the RIC, the difference in this RIC between the relaxed and the deformed geometry, the percentage of strain stored in the RIC and the strain energy.

and three adjacent bonds define a dihedral angle. If desired, hydrogen bonds can be included, which are defined if the distance between the hydrogen atom and the acceptor is larger than 1.3 times the sum of covalent radii but maximally 0.9 times the sum of van der Waals radii. Additionally, the angle between the donor, the hydrogen atom and the acceptor must be at least 90°. The JEDI analysis calculates the values of the internal coordinates, e.g., the lengths of all covalent bonds within the system, at the relaxed and the strained geometries. Subsequently, the elements of the B-matrix are calculated and the transformation of the Hessian matrix from Cartesian coordinates to RICs is carried out. Based on eq. 1, the strain energies in all internal coordinates, ΔE_i, are calculated and finally added up to yield the total harmonic strain energy of the system, ΔE_{harm} (eq. 5). The resulting strain energies are output in form of a text file and a table (cf. Table 1 for an example).

If instead only a subsystem shall be considered, e.g., in a surface/adsorbate system or if calculation time shall be saved in large systems, only the partial Cartesian Hessian is calculated. Since some RICs are neglected, including those that extend over the boundary between the subsystem and the omitted part, the Hessian of the subsystem in RICs is calculated *via* a modification of eq. 4,

$$\mathbf{H_{q,sub}} = \mathbf{P_{sub}}(\mathbf{B_{sub}^{t}})^{+}\mathbf{H_{x,sub}}\mathbf{B_{sub}^{+}}\mathbf{P_{sub}} \; . \tag{6}$$

The result of the partial JEDI analysis is a text file and a table that is analogous to a full JEDI analysis, with the only difference that some internal coordinates are missing.

In addition to the strain analysis produced by JEDI in text form, the user can choose to generate a set of `tcl` scripts for use in the Visual Molecular Dynamics (`VMD`) program.[76] These scripts allow the generation of color-coded structures that indicate the strain within each region of the deformed system visually. The generation of these scripts and their application in `VMD` is highly recommended, because the resulting color-coded structures allow straightforward and chemically intuitive strain analysis at a single glance, which can be augmented by the more detailed strain analysis in text form. Several examples of pictures generated *via* the visualization mode are found in Section 4. The visualization procedure colors the bonds within the system according to the strain found in this region. In the case of covalent bonds, the coloring is straightforward: The highest strain within a covalent bond is defined as red and zero strain as green. The remaining bonds are colored according to the strain energies calculated by JEDI, which leads to fluent transitions of the colors from green through yellow to red. In the case of bond angles and dihedral angles, the strain is divided equally between the covalent bonds involved in them, and the values for a given covalent bond are added up. Hence, separate `tcl` scripts for bond lengths, bond angles and dihedral angles are generated. Finally, all three types of internal coordinates are combined and the strain energies within the bond lengths, bond angles and dihedral angles are mapped onto the bonds, yielding a unified picture of the strain within the system as a fourth `tcl` script. Standard atoms are represented by balls with standard colors, e.g., white for hydrogen and grey for carbon. If present in the system, hydrogen bonds are treated like covalent bonds throughout the JEDI analysis and indicated as dashed, color-coded lines in the visualization. If the JEDI analysis is run on a subsystem, the omitted part of the system is colored black. It is also possible to generate color-coded movies showing the evolution of strain in AIMD simulations by compiling the pictures from each individual step of the trajectory.

The computational demand of the JEDI analysis is determined by the electronic structure calculations of the relaxed and strained geometries and the Hessian matrix. The calculation of the RICs and the B-matrix, the matrix multiplications yielding the strain energies and the visualization procedure have a negligible computational overhead.

4 Examples

In the following, five examples of the JEDI analysis are presented, which demonstrate the versatility of the implementation by applying a diverse set of deformation modes and electronic structure codes. Sections 4.1−4.3 focus on (supra)molecular systems under stretching or compressive forces, whereas strained periodic systems are presented in Sections 4.4 and 4.5.

4.1 Ethane Under Stretching Forces

In a trivial pulling scenario, the carbon atoms of ethane were pulled apart with a force of 4 nN using the External Force is Explicitly Included (EFEI)[77–79] approach, which applies constant forces between user-defined pairs of atoms in an otherwise relaxed geometry optimization. DLPNO-CCSD(T)[75,80–82]/cc-pVTZ[83], as implemented in the `ORCA 5.0.0` program package,[84–86] was used as the underlying electronic structure method.

Stretching the carbon-carbon bond in ethane apart with a force of 4 nN leads to a stretching of this bond by 0.14 Å and to the accumulation of approx. 5.1 kcal/mol of strain energy in this bond (Figure 2). Propagation of strain into other internal coordinates is negligible. On the contrary, insignificant negative energy values on the order of 10^{-2} kcal/mol are found in the bond angles of ethane. Minor negative energy values are caused by the off-diagonal coupling elements in the Hessian ($\mathbf{H}_{ij}$, $i \neq j$) and have been attributed to relaxation effects of certain RICs if another RIC is deformed.[52]

The total strain energy ΔE_{harm} of 5.1 kcal/mol, calculated by JEDI, is approx. 16% higher than $\Delta E_{\text{ab initio}}$, i.e., the energy difference between the relaxed and stretched geometries calculated at the DLPNO-CCSD(T)/cc-pVTZ level of theory. This demonstrates that the harmonic approximation is still valid in ethane stretched apart by a force of 4 nN, although the error is expected to increase quickly with increasing force.

4.2 Dewar and Ladenburg Benzene Under Hydrostatic Compression

As an example of hydrostatic compression, Dewar and Ladenburg benzene were subjected to a pressure of 50 GPa *via* the eXtended Hydrostatic Compression Force Field (X-HCFF)[87] approach as implemented in the `Q-Chem 6.0.0` program package.[88] X-HCFF is a mechanochemical pressure model that uses mechanical forces to compress each atom perpendicular to the molecular van-der-Waals surface. PBE[89]-D3(BJ)[90]/cc-pVDZ[83] was used as the electronic structure method. A scaling factor of 1.0 and 302 tesse-

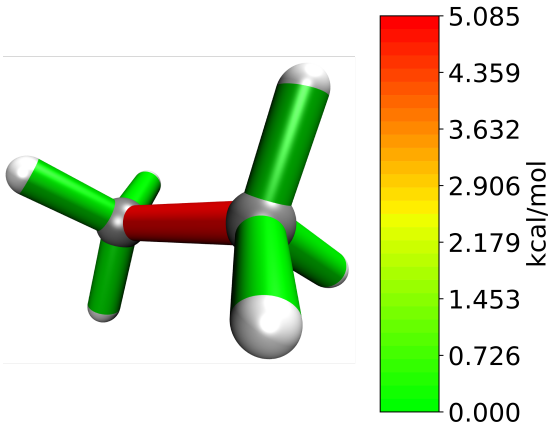

Figure 2: Visual representation of the total strain energy distribution within ethane, in which the carbon-carbon bond is stretched apart by a force of 4nN using the EFEI method.

lation points per atom were chosen as the parameters of X-HCFF.

The application of hydrostatic pressure to Dewar and Ladenburg benzene leads to complex strain distribution patterns (Figure 3). In Dewar benzene, the six-membered ring stores most strain energy. A significant amount of strain can also be observed in the transannular carbon-carbon bond and a low amount of strain is found in the carbon-hydrogen bonds. In Ladenburg benzene, the strain energy is more evenly distributed, with the carbon-carbon bonds connecting the three-membered rings with each other storing the highest amount of strain, followed by the carbon-carbon bonds within the three-membered rings and by the carbon-hydrogen bonds. JEDI calculates a total of 8.1 kcal/mol of strain energy for Dewar benzene and 7.8 kcal/mol for Ladenburg benzene, which demonstrates the slightly higher compressibility of Dewar benzene compared to the more compact Ladenburg benzene. It is interesting to note that ΔE_{harm}, calculated by JEDI, is a few percent lower than $\Delta E_{\text{ab initio}}$: $\Delta E_{\text{ab initio}}$ is 8.7 kcal/mol for Dewar benzene and 8.4 kcal/mol for Ladenburg benzene. This effect is due to the underestimation of the real energy by the harmonic potential in geometries that are more compressed than the equilibrium. Nevertheless, the qualitative agreement between ΔE_{harm} and $\Delta E_{\text{ab initio}}$ validates the JEDI analysis at a pressure as high as 50 GPa and suggests that pressure-induced chemical transformations of the two molecules are not to be expected in this pressure range.

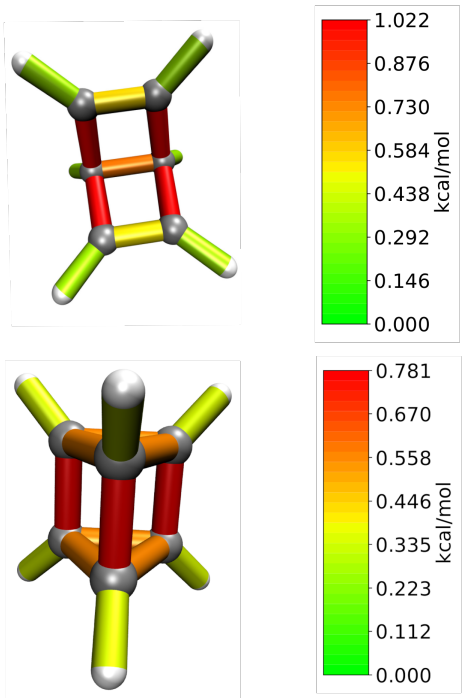

Figure 3: Visual representation of the total strain energy distribution within Dewar (top) and Ladenburg (bottom) benzene under a hydrostatic pressure of 50 GPa applied *via* the X-HCFF method.

4.3 COGEF Calculation of the Cytidine/Guanosine Base Pair

To demonstrate the capability of JEDI to analyze strain in a supramolecular complex, the hydrogen bonds of a cytidine/guanosine base pair were stretched apart using the COnstrained Geometries Simulate External Forces (COGEF)[91,92] approach. COGEF is arguably the most widely used approach in quantum mechanochemistry and simulates mechanical forces by constraining user-defined interatomic distances during a geometry optimization. In the present case, each hydrogen bond was elongated by 0.1 Å. B3LYP[93–95]-D3(BJ)[90]/6-311++G(d),[96,97] as implemented in the `Gaussian16` program package,[98] was used as the electronic structure method.

Intuitively, only the hydrogen bonds between the two bases store a noteworthy amount of strain (Figure 4). No significant propagation of strain into other types of RICs or other parts of the base pair can be observed. Despite the chemical difference between the hydrogen bonds, all three of them store between 0.18 and 0.20 kcal/mol of strain, with the total harmonic strain energy amounting to 0.56 kcal/mol. ΔE_{harm} overestimates $\Delta E_{\text{ab initio}}$ by approx. 15%, justifying the harmonic approximation. The small amount of strain stored in the hydrogen bonds is caused by their "softness" compared to much stiffer covalent bonds.

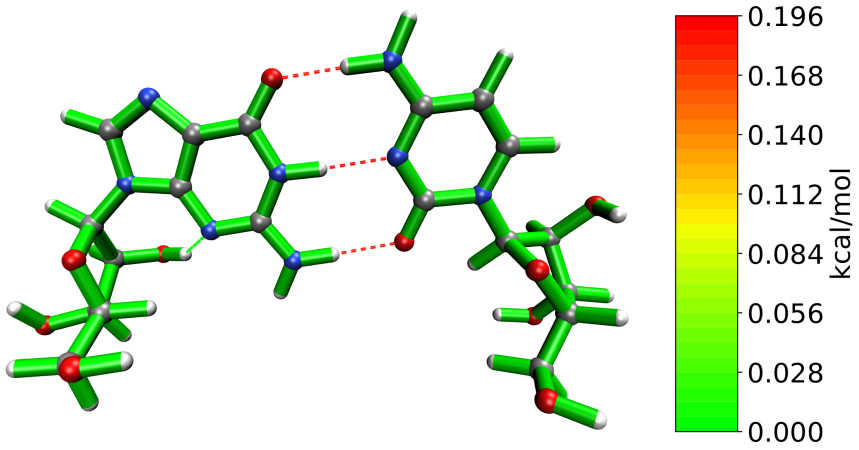

Figure 4: Visual representation of the total strain energy distribution within the cytidine/guanosine base pair, in which the hydrogen bonds (red dashed lines) are elongated by 0.1 Å. The relaxed intramolecular hydrogen bond in guanosine is represented as a green dotted line.

4.4 Partial Strain Analysis in Hydrogen Cyanide

As an example of a partial strain analysis in a periodic system, we considered the HCN crystal, which crystallizes in long chains.[99,100] To induce strain, one of the HCN molecules was displaced by 0.1 Å in x-direction, i.e., perpendicular to the direction of the HCN chains. Additionally, the C−H bond of this molecule was elongated by 0.1 Å. An enlarged unit cell with 16 HCN molecules was chosen to enable a substructure analysis, in which one half of the molecules is omitted. PBE-D3-BJ[89,90] as implemented in GPAW[101] 21.1.0 was used as the density functional, the energy cutoff was set to 700 eV and a k-point grid of 3x2x2 was chosen. The size of the unit cell was fixed in this simulation. Work on a version of JEDI that allows variable unit cell size has begun in our group.

The distortion introduced in the HCN crystal leads to a total harmonic strain energy of 3.39 kcal/mol, which is approx. 15% higher than $E_{\text{ab initio}}$. As an example of a JEDI analysis on a subset of RICs, the strain energy distribution within the bond angles is shown in Figure 5. In this type of RICs, the strain is localized within the HCN chain that contains the displaced HCN molecule, and most strain is localized in those bond angles that include the hydrogen bonds. The parts of the system that are omitted in the partial strain analysis are colored black. Omitting a part of the system in the JEDI analysis has the benefit of saving computation time. In addition, we expect this feature to become a useful tool in strain analysis of adsorbates.

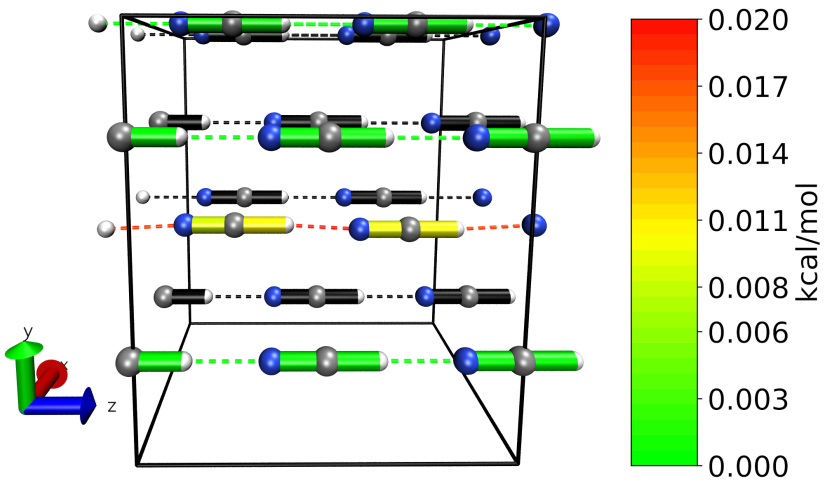

Figure 5: Visual representation of the partial strain energy distribution in the bond angles of the HCN crystal, in which one HCN molecule was displaced by 0.1 Å in x-direction. Additionally, the C−H bond of this molecule was elongated by 0.1 Å. Molecules omitted in the partial strain analysis are shown with black bonds. The black lines indicate the periodically repeating simulation box.

4.5 Dynamic Strain Analysis in Graphene

Dynamic strain analyses can be carried out with JEDI by starting an *ab initio* Molecular Dynamics (AIMD) simulation from a relaxed geometry and considering each time step as a strained geometry. In this case, JEDI quantifies the additional potential energy in terms of strain throughout the AIMD trajectory. To demonstrate such a dynamic strain analysis in a periodic system, an *NVT* simulation of graphene with an integration time step of 0.5 fs was carried out. During the first 1,000 time steps, the system was heated from 0 K to 400 K, after which 72,000 time steps were simulated at 400 K. PBE-D3-BJ[89,90] as implemented in VASP[102–104] 6.3.0 was used as the level of theory. A k-point grid of 6x6x1 and an energy cutoff of 450 eV were chosen.

A color-coded movie of the strain due to thermal oscillations is given in the Supporting Information. Snapshots showing the momentary strain at three representative points of the trajectory are shown in Figure 6. As can be learned from these types of visualization, thermal oscillations lead to changes in C−C bond lengths and to out-of-plane bendings of the graphene sheet, which in turn result in a complex time-dependent strain distribution pattern. It is important to note that only the potential part of the energy is quantified by JEDI and the changes in kinetic energy are ignored, hence, JEDI analyses on AIMD trajectories yield semi-quantitative insights into the dynamic behavior of strain. In the past, such dynamical studies have enabled discussions of the mechancial stability of a tightening polymer knot[54] and the feasibility of force-induced retro-click reactions.[56]

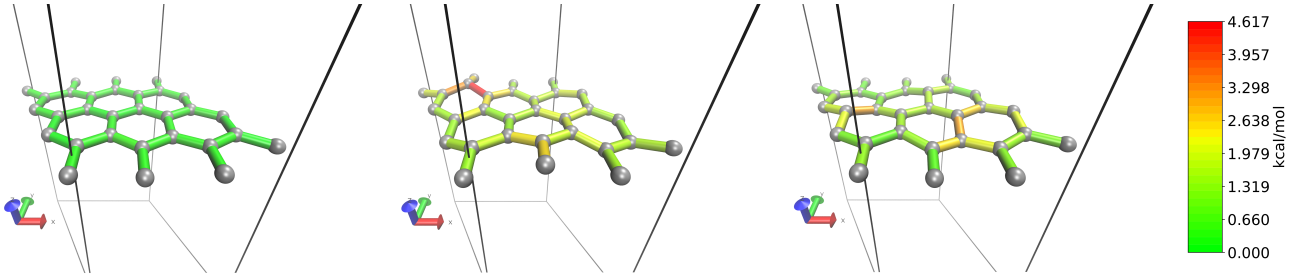

Figure 6: Snapshots of the strain distribution calculated with JEDI during an *NVT* simulation at 0 ps (left), 340 ps (middle) and 970 ps (right).

5 Summary and Outlook

In this paper, we have presented a flexible implementation of the Judgement of Energy DIstribution (JEDI) analysis that allows the calculation of the mechanical strain energy distribution within molecules, supramolecular clusters and periodic systems under various types of deformation. Based on the harmonic approximation, a strain energy value is calculated for each bond length, bond angle, dihedral angle and, possibly, hydrogen bond within a mechanically deformed system. The underlying calculations are typically carried out using Density Functional Theory (DFT) or wavefunction-based methods, ensuring quantum mechanical accuracy. Calculations of the strain within substructures of a chemical system are possible, allowing strain analyses of adsorbates or of systems that would otherwise be too costly to analyze fully. Dynamical strain analyses on the basis of *ab initio* Molecular Dynamics simulations are possible, in which the geometry found at each time step of the trajectory is considered as a strained geometry. Maximum versatility of the code is guaranteed by the implementation into the Atomic Simulation Environment (`ASE`) program package, which establishes an interface to various electronic structure codes, and a visual representation of the force-bearing scaffold is generated automatically *via* the Visual Molecular Dynamics (`VMD`) program.

We hope that the chemically diverse examples presented here spark the readers' interest in applying the JEDI analysis to a range of problems in mechano- and high-pressure chemistry, materials science, mechanobiology and beyond. While the range of applied computer codes, example molecules and materials, and deformation modes discussed in Section 4 is necessarily limited, in principle there is no limit to the possible application scenarios of JEDI, as long as the harmonic approximation is valid. We are excited to see to what problems the JEDI analysis will be applied in the future and what new insights will be gained with it.

Acknowledgements

We acknowledge financial support through the APF project 'Materials on Demand' within the 'Humans on Mars' Initiative funded by the Federal State of Bremen and the University of Bremen. We thank Chieh-Min Hsieh and Noah Wolf, University of Bremen, Germany, for fruitful discussions.

Supporting Information Available

Color-coded movie of the dynamic JEDI analysis of graphene; JEDI scripts for all examples.

Data Availability

The data that support the findings of this study are openly available in the Supporting Information and on https://github.com/neudecker-group/jedi.

References

[1] Traeger, H.; Kiebala, D. J.; Weder, C.; Schrettl, S. From Molecules to Polymers - Harnessing Inter- and Intramolecular Interactions to Create Mechanochromic Materials. *Macromol. Rapid Commun.* **2021**, *42*, 2000573.

[2] He, S.; Stratigaki, M.; Centeno, S. P.; Dreuw, A.; Göstl, R. Tailoring the Properties of Optical Force Probes for Polymer Mechanochemistry. *Chem. Eur. J.* **2021**, *64*, 15889–15897.

[3] Aziz, A.; Sidat, A.; Talati, P.; Crespo-Otero, R. Understanding the Solid State Luminescence and Piezochromic Properties in Polymorphs of an Anthracene Derivative. *Phys. Chem. Chem. Phys.* **2022**, *24*, 2832–2842.

[4] Irii, S.; Ogaki, T.; Miyashita, H.; Nobori, K.; Ozawa, Y.; Abe, M.; Sato, H.; Ohta, E.; Matsui, Y.; Ikeda, H. Remarkable Piezofluorochromism of an Organoboron Complex Containing [2.2]Paracyclophane. *Tetrahedron Lett.* **2022**, *101*, 153913.

[5] Liu, J.; Du, G.; Liang, N.; Yang, L.; Feng, Y.; Chen, Y.; Yao, C.-J. Tunable Near-Infrared Piezochromic Luminescence by Effective Substituent Modification of D–A Structures. *J. Mater. Chem. C* **2023**, *11*, 8609–8615.

[6] De Bo, G. Polymer Mechanochemistry and the Emergence of the Mechanophore Concept. *Macromolecules* **2020**, *53*, 7615–7617.

[7] Jung, S.; Yoon, H. J. Heterocyclic Mechanophores in Polymer Mechanochemistry. *Synlett* **2022**, *33*, 863–874.

[8] Versaw, B. A.; Zeng, T.; Hu, X.; Robb, M. J. Harnessing the Power of Force: Development of Mechanophores for Molecular Release. *J. Am. Chem. Soc.* **2021**, *143*, 21461–21473.

[9] Binder, W. H. The "labile" Chemical Bond: A Perspective on Mechanochemistry in Polymers. *Polymer* **2020**, *202*, 122639.

[10] Ghanem, M. A.; Basu, A.; Behrou, R.; Boechler, N.; Boydston, A. J.; Craig, S. L.; Lin, Y.; Lynde, B. E.; Nelson, A.; Shen, H.; Storti, D. W. The Role of Polymer Mechanochemistry in Responsive Materials and Additive Manufacturing. *Nat. Rev. Mater.* **2020**, DOI: 10.1038/s41578–020–00249–w.

[11] Küng, R.; Göstl, R.; Schmidt, B. M. Release of Molecular Cargo from Polymer Systems by Mechanochemistry. *Chem. Eur. J.* **2022**, *28*, e202103860.

[12] Shen, H.; Cao, Y.; Lv, M.; Sheng, Q.; Zhang, Z. Polymer Mechanochemistry for Release of Small Cargoes. *Chem. Commun.* **2022**, *58*, 4813–4824.

[13] Lloyd, E. M.; Vakil, J. R.; Yao, Y.; Sottos, N. R.; Craig, S. L. Covalent Mechanochemistry and Contemporary Polymer Network Chemistry: A Marriage in the Making. *J. Am. Chem. Soc.* **2023**, DOI: jacs.2c09623.

[14] Gütlich, P.; Ksenofontov, V.; Gaspar, A. B. Pressure Effect Studies on Spin Crossover Systems. *Coord. Chem. Rev.* **2005**, *249*, 1811–1829.

[15] Hogue, R. W.; Singh, S.; Brooker, S. Spin Crossover in Discrete Polynuclear Iron(II) Complexes. *Chem. Soc. Rev.* **2018**, *47*, 7303–7338.

[16] Bondì, L.; Brooker, S.; Totti, F. Accurate Prediction of Pressure and Temperature T 1/2 Variation in Solid State Spin Crossover by Ab Initio Methods: The [CoII(Dpzca)2] Case. *J. Mater. Chem. C* **2021**, *9*, 14256–14268.

[17] Davis, D. A.; Hamilton, A.; Yang, J.; Cremar, L. D.; van Gough, D.; Potisek, S. L.; Ong, M. T.; Braun, P. V.; Martínez, T. J.; White, S. R.; Moore, J. S.; Sottos, N. R. Force-Induced Activation of Covalent Bonds in Mechanoresponsive Polymeric Materials. *Nature* **2009**, *459*, 68–72.

[18] Kabb, C. P.; O'Bryan, C. S.; Morley, C. D.; Angelini, T. E.; Sumerlin, B. S. Anthracene-Based Mechanophores for Compression-Activated Fluorescence in Polymeric Networks. *Chem. Sci.* **2019**, *10*, 7702–7708.

[19] Binnig, G.; Quate, C. F. Atomic Force Microscope. *Phys. Rev. Lett.* **1986**, *56*, 930–933.

[20] Neuman, K. C.; Nagy, A. Single-Molecule Force Spectroscopy: Optical Tweezers, Magnetic Tweezers and Atomic Force Microscopy. *Nat. Methods* **2008**, *5*, 491–505.

[21] Hinterdorfer, P.; Dufrêne, Y. F. Detection and Localization of Single Molecular Recognition Events Using Atomic Force Microscopy. *Nat. Methods* **2006**, *3*, 347–355.

[22] Fisher, T. E.; Marszalek, P. E.; Fernandez, J. M. Stretching Single Molecules into Novel Conformations Using the Atomic Force Microscope. *Nat. Struct. Biol.* **2000**, *7*, 719–724.

[23] Cravotto, G.; Cintas, P. Power Ultrasound in Organic Synthesis: Moving Cavitational Chemistry from Academia to Innovative and Large-Scale Applications. *Chem. Soc. Rev.* **2006**, *35*, 180–196.

[24] Cravotto, G.; Cintas, P. Forcing and Controlling Chemical Reactions with Ultrasound. *Angew. Chem. Int. Ed.* **2007**, *46*, 5476–5478.

[25] May, P. A.; Moore, J. S. Polymer Mechanochemistry: Techniques to Generate Molecular Force via Elongational Flows. *Chem. Soc. Rev.* **2013**, *42*, 7497–7506.

[26] Cintas, P.; Cravotto, G.; Barge, A.; Martina, K. Interplay Between Mechanochemistry and Sonochemistry. *Top. Curr. Chem.* **2015**, *369*, 239–284.

[27] Martínez, R. F.; Cravotto, G.; Cintas, P. Organic Sonochemistry: A Chemist's Timely Perspective on Mechanisms and Reactivity. *J. Org. Chem.* **2021**, DOI: 10.1021/acs.joc.1c00805.

[28] Rodríguez, B.; Bruckmann, A.; Rantanen, T.; Bolm, C. Solvent-Free Carbon-Carbon Bond Formations in Ball Mills. *Adv. Synth. Catal.* **2007**, *349*, 2213–2233.

[29] Bolm, C.; Hernández, J. G. Mechanochemistry of Gaseous Reactants. *Angew. Chem. Int. Ed.* **2019**, *58*, 3285–3299.

[30] Li, B.; Ji, C.; Yang, W.; Wang, J.; Yang, K.; Xu, R.; Liu, W.; Cai, Z.; Chen, J.; kwang Mao, H. Diamond Anvil Cell Behavior up to 4 Mbar. *Proc. Nat. Acad. Sci. U.S.A.* **2018**, *115*, 1713–1717.

[31] Katrusiak, A. Lab in a DAC - High-pressure Crystal Chemistry in a Diamond-Anvil Cell. *Acta Cryst. B* **2019**, *75*, 918–926.

[32] Stauch, T.; Dreuw, A. Advances in Quantum Mechanochemistry: Electronic Structure Methods and Force Analysis. *Chem. Rev.* **2016**, *116*, 14137–14180.

[33] Makarov, D. E. Perspective: Mechanochemistry of Biological and Synthetic Molecules. *J. Chem. Phys.* **2016**, *144*, 030901.

[34] Kochhar, G. S.; Heverly-Coulson, G. S.; Mosey, N. J. Theoretical Approaches for Understanding the Interplay Between Stress and Chemical Reactivity. *Top. Curr. Chem.* **2015**, *369*, 37–96.

[35] Ribas-Arino, J.; Marx, D. Covalent Mechanochemistry: Theoretical Concepts and Computational Tools with Applications to Molecular Nanomechanics. *Chem. Rev.* **2012**, *112*, 5412–5487.

[36] Beyer, M. K.; Clausen-Schaumann, H. Mechanochemistry: The Mechanical Activation of Covalent Bonds. *Chem. Rev.* **2005**, *105*, 2921–2948.

[37] Zhang, M.; De Bo, G. Mechanical Susceptibility of a Rotaxane. *J. Am. Chem. Soc.* **2019**, *141*, 15879–15883.

[38] Zhang, M.; De Bo, G. Impact of a Mechanical Bond on the Activation of a Mechanophore. *J. Am. Chem. Soc.* **2018**, *140*, 12724–12727.

[39] Avdoshenko, S. M.; Konda, S. S. M.; Makarov, D. E. On the Calculation of Internal Forces in Mechanically Stressed Polyatomic Molecules. *J. Chem. Phys.* **2014**, *141*, 134115.

[40] Jones, L. H.; Swanson, B. I. Interpretation of Potential Constants: Application to Study of Bonding Forces in Metal Cyanide Complexes and Metal Carbonyls. *Acc. Chem. Res.* **1976**, *9*, 128–134.

[41] Grunenberg, J.; Streubel, R.; von Frantzius, G.; Marten, W. The Strongest Bond in the Universe? Accurate Calculation of Compliance Matrices for the Ions N2H+, HCO+, and HOC+. *J. Chem. Phys.* **2003**, *119*, 165–169.

[42] Brandhorst, K.; Grunenberg, J. Characterizing Chemical Bond Strengths Using Generalized Compliance Constants. *ChemPhysChem* **2007**, *8*, 1151–1156.

[43] Brandhorst, K.; Grunenberg, J. How Strong Is It? The Interpretation of Force and Compliance Constants as Bond Strength Descriptors. *Chem. Soc. Rev.* **2008**, *37*, 1558–1567.

[44] Brandhorst, K.; Grunenberg, J. Efficient Computation of Compliance Matrices in Redundant Internal Coordinates from Cartesian Hessians for Nonstationary Points. *J. Chem. Phys.* **2010**, *132*, 184101.

[45] Stacklies, W.; Vega, M. C.; Wilmanns, M.; Gräter, F. Mechanical Network in Titin Immunoglobulin from Force Distribution Analysis. *PLoS Comput. Biol.* **2009**, *5*, e1000306.

[46] Stacklies, W.; Xia, F.; Gräter, F. Dynamic Allostery in the Methionine Repressor Revealed by Force Distribution Analysis. *PLoS Comput. Biol.* **2009**, *5*, e1000574.

[47] Gräter, F. In *Modeling of Molecular Properties*; Comba, P., Ed.; Wiley-VCH: Weinheim, 2011; pp 301–310.

[48] Stacklies, W.; Seifert, C.; Gräter, F. Implementation of Force Distribution Analysis for Molecular Dynamics Simulations. *BMC Bioinf.* **2011**, *12*, 101.

[49] Costescu, B. I.; Gräter, F. Time-Resolved Force Distribution Analysis. *BMC Biophys.* **2013**, *6*, 5.

[50] Wheeler, S. E.; Houk, K. N.; von Ragué Schleyer, P.; Allen, W. D. A Hierarchy of Homodesmotic Reactions for Thermochemistry. *J. Am. Chem. Soc.* **2009**, *131*, 2547–2560.

[51] Colwell, C. E.; Price, T. W.; Stauch, T.; Jasti, R. Strain Visualization for Strained Macrocycles. *Chem. Sci.* **2020**, *11*, 3923–3930.

[52] Stauch, T.; Dreuw, A. A Quantitative Quantum-Chemical Analysis Tool for the Distribution of Mechanical Force in Molecules. *J. Chem. Phys.* **2014**, *140*, 134107.

[53] Stauch, T.; Dreuw, A. On the Use of Different Coordinate Systems in Mechanochemical Force Analyses. *J. Chem. Phys.* **2015**, *143*, 074118.

[54] Stauch, T.; Dreuw, A. Knots "Choke Off" Polymers upon Stretching. *Angew. Chem. Int. Ed.* **2016**, *55*, 811–814.

[55] Stauch, T.; Dreuw, A. Polymere Werden Beim Strecken Durch Knoten Abgeschnürt. *Angew. Chem.* **2016**, *128*, 822–825.

[56] Stauch, T.; Dreuw, A. Force-Induced Retro-Click Reaction of Triazoles Competes with Adjacent Single-Bond Rupture. *Chem. Sci.* **2017**, *8*, 5567–5575.

[57] Balzaretti, F.; von Einem, M.; Gerhards, L.; Dononelli, W.; Stauch, T.; Klüner, T.; Köppen, S. Charge-Transfer Promoted Fixation of Glyphosate on TiO2 - a Multiscale Approach. *ChemRxiv* **2021**, DOI: 10.26434/chemrxiv.14465436.v1.

[58] Scheurer, M.; Dreuw, A.; Head-Gordon, M.; Stauch, T. The Rupture Mechanism of Rubredoxin Is More Complex than Previously Thought. *Chem. Sci.* **2020**, *11*, 6036–6044.

[59] Stauch, T.; Günther, B.; Dreuw, A. Can Strained Hydrocarbons Be "Forced" To Be Stable? *J. Phys. Chem. A* **2016**, *120*, 7198–7204.

[60] Slavov, C.; Yang, C.; Heindl, A. H.; Stauch, T.; Wegner, H. A.; Dreuw, A.; Wachtveitl, J. Twist and Return - Induced Ring Strain Triggers Quick Relaxation of a (Z)-Stabilized Cyclobisazobenzene. *J. Phys. Chem. Lett.* **2018**, *9*, 4776–4781.

[61] Mier, L. J.; Adam, G.; Kumar, S.; Stauch, T. The Mechanism of Flex-Activation in Mechanophores Revealed By Quantum Chemistry. *ChemPhysChem* **2020**, *21*, 2402–2406.

[62] Kumar, S.; Stauch, T. The Activation Efficiency of Mechanophores Can Be Modulated by Adjacent Polymer Composition. *RSC Adv.* **2021**, *11*, 7391–7396.

[63] Kumar, S.; Zeller, F.; Stauch, T. A Two-Step Baromechanical Cycle for Repeated Activation and Deactivation of Mechanophores. *J. Phys. Chem. Lett.* **2021**, *12*, 9470–9474.

[64] Larsen, A. H. et al. The Atomic Simulation Environment - a Python Library for Working with Atoms. *J. Phys.: Condens. Matter* **2017**, *29*, 273002.

[65] Stauch, T.; Dreuw, A. Quantum Chemical Strain Analysis For Mechanochemical Processes. *Acc. Chem. Res.* **2017**, *50*, 1041–1048.

[66] Stauch, T.; Dreuw, A. Predicting the Efficiency of Photoswitches Using Force Analysis. *J. Phys. Chem. Lett.* **2016**, *7*, 1298–1302.

[67] Stauch, T.; Dreuw, A. Stiff-Stilbene Photoswitch Ruptures Bonds Not by Pulling but by Local Heating. *Phys. Chem. Chem. Phys.* **2016**, *18*, 15848–15853.

[68] Wilson, E. B.; Decius, J. C.; Cross, P. C. *Molecular Vibrations. The Theory of Infrared and Raman Vibrational Spectra*; Dover Publications Inc: Mineola, New York, 1955.

[69] Bakken, V.; Helgaker, T. The Efficient Optimization of Molecular Geometries Using Redundant Internal Coordinates. *J. Chem. Phys.* **2002**, *117*, 9160–9174.

[70] Stauch, T. Quantum Chemical Modeling of Molecules under Pressure. *Int. J. Quantum Chem.* **2021**, *121*, e26208.

[71] Zeller, F.; Hsieh, C.-M.; Dononelli, W.; Neudecker, T. Computational High-Pressure Chemistry: Ab Initio Simulations of Atoms, Molecules and Extended Materials in the Gigapascal Regime. *ChemRxiv* **2023**, DOI: 10.26434/chemrxiv–2023–nr314.

[72] Hohenberg, P.; Kohn, W. Inhomogeneous Electron Gas. *Phys. Rev.* **1964**, *136*, 864–871.

[73] Kohn, W.; Sham, L. J. Self-Consistent Equations Including Exchange and Correlation Effects. *Phys. Rev.* **1965**, *140*, 1133–1138.

[74] Møller, C.; Plesset, M. S. Note on an Approximation Treatment for Many-Electron Systems. *Phys. Rev.* **1934**, *46*, 618–622.

[75] Coester, F.; Kümmel, H. Short-Range Correlations in Nuclear Wave Functions. *Nucl. Phys.* **1960**, *17*, 477–485.

[76] Humphrey, W.; Dalke, A.; Schulten, K. VMD: Visual Molecular Dynamics. *J. Mol. Graphics* **1996**, *14*, 33–38.

[77] Ribas-Arino, J.; Shiga, M.; Marx, D. Understanding Covalent Mechanochemistry. *Angew. Chem. Int. Ed.* **2009**, *48*, 4190–4193.

[78] Ong, M. T.; Leiding, J.; Tao, H.; Virshup, A. M.; Martínez, T. J. First Principles Dynamics and Minimum Energy Pathways for Mechanochemical Ring Opening of Cyclobutene. *J. Am. Chem. Soc.* **2009**, *131*, 6377–6379.

[79] Wolinski, K.; Baker, J. Theoretical Predictions of Enforced Structural Changes in Molecules. *Mol. Phys.* **2009**, *107*, 2403–2417.

[80] Riplinger, C.; Neese, F. An Efficient and near Linear Scaling Pair Natural Orbital Based Local Coupled Cluster Method. *J. Chem. Phys.* **2013**, *138*, 034106.

[81] Purvis III, G. D.; Bartlett, R. J. A Full Coupled-Cluster Singles and Doubles Model: The Inclusion of Disconnected Triples. *J. Chem. Phys.* **1982**, *76*, 1910–1918.

[82] Raghavachari, K.; Trucks, G. W.; Pople, J. A.; Head-Gordon, M. A Fifth-Order Perturbation Comparison of Electron Correlation Theories. *Chem. Phys. Lett.* **1989**, *157*, 479–483.

[83] Dunning, T. H. Gaussian Basis Sets for Use in Correlated Molecular Calculations. I. The Atoms Boron through Neon and Hydrogen. *J. Chem. Phys.* **1989**, *90*, 1007–1023.

[84] Neese, F. The ORCA Program System. *WIREs Comput. Mol. Sci.* **2012**, *2*, 73–78.

[85] Neese, F. Software Update: The ORCA Program System, Version 4.0. *WIREs Comput. Mol. Sci.* **2018**, *8*, e1327.

[86] Neese, F. Software Update: The ORCA Program System—Version 5.0. *WIREs Comput. Mol. Sci.* **2022**, *12*, e1606.

[87] Stauch, T. A Mechanochemical Model for the Simulation of Molecules and Molecular Crystals under Hydrostatic Pressure. *J. Chem. Phys.* **2020**, *153*, 134503.

[88] Epifanovsky, E. et al. Software for the Frontiers of Quantum Chemistry: An Overview of Developments in the Q-Chem 5 Package. *J. Chem. Phys.* **2021**, *155*, 084801.

[89] Perdew, J. P.; Burke, K.; Ernzerhof, M. Generalized Gradient Approximation Made Simple. *Phys. Rev. Lett.* **1996**, *77*, 3865–3868.

[90] Grimme, S.; Antony, J.; Ehrlich, S.; Krieg, H. A Consistent and Accurate Ab Initio Parametrization of Density Functional Dispersion Correction (DFT-D) for the 94 Elements H-Pu. *J. Chem. Phys.* **2010**, *132*, 154104.

[91] Nikitina, E. A.; Khavryutchenko, V. D.; Sheka, E. F.; Barthel, H.; Weis, J. Deformation of Poly(Dimethylsiloxane) Oligomers under Uniaxial Tension: Quantum Chemical View. *J. Phys. Chem. A* **1999**, *103*, 11355–11365.

[92] Beyer, M. K. The Mechanical Strength of a Covalent Bond Calculated by Density Functional Theory. *J. Chem. Phys.* **2000**, *112*, 7307–7312.

[93] Becke, A. D. Density-Functional Exchange-Energy Approximation with Correct Asymptotic Behavior. *Phys. Rev. A* **1988**, *38*, 3098–3100.

[94] Lee, C.; Yang, W.; Parr, R. G. Development of the Colle-Salvetti Correlation-Energy Formula into a Functional of the Electron Density. *Phys. Rev. B* **1988**, *37*, 785–789.

[95] Becke, A. D. A New Mixing of Hartree-Fock and Local Density-Functional Theories. *J. Chem. Phys.* **1993**, *98*, 1372–1377.

[96] Hehre, W. J.; Ditchfield, R.; Pople, J. A. Self—Consistent Molecular Orbital Methods. XII. Further Extensions of Gaussian—Type Basis Sets for Use in Molecular Orbital Studies of Organic Molecules. *J. Chem. Phys.* **1972**, *56*, 2257–2261.

[97] Krishnan, R.; Binkley, J. S.; Seeger, R.; Pople, J. A. Self-Consistent Molecular Orbital Methods. XX. A Basis Set for Correlated Wave Functions. *J. Chem. Phys.* **1980**, *72*, 650–654.

[98] Frisch, M. J. et al. Gaussian16 Revision C.01. 2016.

[99] Dulmage, W. J.; Lipscomb, W. N. The Crystal Structures of Hydrogen Cyanide, HCN. *Acta Cryst.* **1951**, *4*, 330–334.

[100] MacKenzie, G. A.; Pawley, G. S. A Neutron Scattering Study of DCN. *J. Chem. Phys. C: Solid State Phys.* **1979**, *12*, 2715–2735.

[101] Mortensen, J. J.; Hansen, L. B.; Jacobsen, K. W. Real-Space Grid Implementation of the Projector Augmented Wave Method. *Phys. Rev. B* **2005**, *71*, 035109.

[102] Kresse, G.; Hafner, J. Ab Initio Molecular-Dynamics Simulation of the Liquid-Metalamorphous-Semiconductor Transition in Germanium. *Phys. Rev. B* **1994**, *49*, 14251–14269.

[103] Kresse, G.; Furthmüller, J. Efficiency of Ab-Initio Total Energy Calculations for Metals and Semiconductors Using a Plane-Wave Basis Set. *Comput. Mater. Sci.* **1996**, *6*, 15–50.

[104] Kresse, G.; Furthmüller, J. Efficient Iterative Schemes for Ab Initio Total-Energy Calculations Using a Plane-Wave Basis Set. *Phys. Rev. B* **1996**, *54*, 11169–11186.